Electronic Supplementary Material (ESI) for Materials Chemistry Frontiers.

Supplementary Information

Self-Assembled Nanoparticles Formed via Complementary Nucleobase Pair Interactions between Drugs and Nanocarriers for Highly Efficient Tumor-Selective Chemotherapy

Fasih Bintang Ilhami,[a#] Ai Chung,[a#] Yihalem Abebe Alemayehu,[a#] Ai-Wei Lee,[de] Jem-Kun Chen,[bc] Juin-Yih Lai[abf] and Chih-Chia Cheng[ab]*

a. Graduate Institute of Applied Science and Technology, National Taiwan University of Science and Technology, Taipei 10607, Taiwan.
b. Advanced Membrane Materials Research Center, National Taiwan University of Science and Technology, Taipei 10607, Taiwan.
c. Department of Materials Science and Engineering, National Taiwan University of Science and Technology, Taipei 10607, Taiwan.
d. Department of Anatomy and Cell Biology & Taipei Heart Institute, Taipei Medical University, Taipei, 11031, Taiwan.
e. Cardiovascular Research Center, Taipei Medical University Hospital, Taipei, 11031, Taiwan.
f. R&D Center for Membrane Technology, Chung Yuan Christian University, Chungli, Taoyuan 32043, Taiwan.

# These authors contributed equally to this work.

* Corresponding Author

E-mail: cccheng@mail.ntust.edu.tw

Experimental Section

Chemicals and materials

Rhodamine 6G (dye content 99 %), poly(propylene glycol) diacrylate (number-average molecular weight, *M*n: ~800 g/mol), uracil (> 99%), adenine (> 99.5% purity), dimethylformamide (DMF), methanol and potassium tertbutoxide were purchased from Sigma-Aldrich (St. Louis, MO, USA) or Acros Organics (Geel, Belgium) at the highest purity available; all other chemicals and reagents were purchased from Sigma-Aldrich at the highest purity available. The synthesis and structural characterization of BU-PPG and A-MA were performed as described in detail in our previous studies.[16,37]

Synthesis of A-Propylamine

A-MA (1 g, 0.0045 mol) and 1,3-diaminopropane (10 g, 0.135 mol) were solved in methanol (100 mL) and reacted at room temperature (~20–25 °C) with stirring under a slow stream of nitrogen until the ester carbonyl peak of A-MA (at 1720-1730 cm^{-1}) completely disappeared from the Fourier transform infrared (FTIR) spectra of the monitored samples. Subsequently, the mixture was filtered through filter paper using a Büchner funnel via vacuum suction, and the resulting solution was subjected to vacuum distillation to remove excess 1,3-diaminopropane and methanol. Finally, the residual oil sample was washed several times with tetrahydrofuran and acetone to obtain A-Propylamine as a yellowish white powder, yield 86% (1.02 g).

Synthesis of A-R6G

R6G (0.5 g, 0.001 mol) and A-Propylamine (1.7 g, 0.006 mol) were solved in methanol (50 mL) in a two-neck flask equipped with a stirrer and maintained at 50 °C for one week under a

nitrogen atmosphere. Methanol was removed using a rotary evaporator, then chloroform was added to the crude oil sample and stirred at room temperature for 1 h. The insoluble materials were removed by filtration through a Buchner funnel and the remaining chloroform was removed using a rotary evaporator. Subsequently, the crude sample was refluxed with diethyl ether and cooled to give a reddish-brown precipitate. Finally, the product was washed twice with acetone to obtain A-R6G as a pink powder, yield 75% (0.5 g).

Characterization

Fourier transform infrared (FTIR) and proton/carbon nuclear magnetic resonance spectra (^{1}H and ^{13}C NMR)*:* The synthesized materials were initially characterized using FTIR on a PerkinElmer Spectrum Two IR spectrometer over the scan range from 600-4000 cm^{-1}. Background spectra were obtained to eliminate the effects of atmospheric moisture and carbon dioxide. To elucidate the structures of the products, NMR spectra were recorded using a Bruker AVIII instrument (Billerica, MA, USA) at 500 MHz in deuterated solvent using the standard reference tetramethylsilane (TMS).

Mass spectrometry*:* molecular weights were analyzed in methanol using electrospray ionization-mass spectrometry (ESI-MS; VG Platform, Fisons Instruments, Altrincham, UK). Accurate mass spectra were collected in both positive and negative ion mode.

Elemental analysis*:* elemental CHN analyses were obtained using a Flash 2000 Elemental Analyzer (Thermo Fisher Scientific, Voltaweg, the Netherlands). Simultaneous determination of the elements C, H and N was based on full combustion of the samples at up to 1200 °C in an oxygen atmosphere.

Photoluminescence (PL) spectroscopy: the fluorescence intensity of R6G, A-R6G, and R6G-loaded and A-R6G-loaded BU-PPG nanoparticles were determined using a luminescence spectrometer (Hitachi F4500, Tokyo, Japan), using a Xenon lamp at 25 °C.

Dynamic light scattering (DLS) and zeta potentials: the surface charge, hydrodynamic diameter, size distribution and polydispersity index (PDI) of aqueous solutions of R6G, A-R6G and the polymers were obtained with a Nano Brook 90Plus PALS instrument (Brookhaven, Holtsville, NY, USA) equipped with a 632 nm He-Ne laser beam and at a fixed scattering angle of 90°. All samples were incubated at 25 °C for at least 30 min before DLS measurements.

Atomic force microscopy (AFM) and scanning electron microscopy (SEM): R6G, A-R6G, and R6G-loaded and A-R6G-loaded BU-PPG nanoparticles were prepared by spin coating and vacuum drying at 25 °C for 24 h and their morphologies were assessed using a tapping mode AFM (NX10; AFM Park Systems, Suwon, South Korea) equipped with a standard commercial probe made of silicon (125 nm). The elemental compositions and morphology of the samples were determined using a field-emission SEM (JSM-6500F, JEOL, Tokyo, Japan).

Preparation of R6G-loaded and A-R6G-loaded BU-PPG nanoparticles

R6G or A-R6G were encapsulated into BU-PPG using a dialysis method. Briefly, the polymer dissolved in phosphate-buffered saline (PBS; pH 7.4, 10 mM) was added to R6G or A-R6G solution at various polymer/drug ratios (ranging 0.1 to 1 mg), stirred for 24 h, then purified by dialysis against PBS in 1000 Da molecular-weight cut-off dialysis tubing for 24 h. The particle size distributions of R6G-loaded and A-R6G-loaded nanoparticles were characterized by DLS and AFM. DLS particle size measurements were used to evaluate the pH-responsiveness of R6G-loaded and A-R6G-loaded nanoparticles at pH 5.5, 6.5 and 7.4. The drug loading content (DLC)

and loading efficiency (DLE) were analyzed using an UV-Vis spectrophotometer at λ = 525 nm (the absorbance intensity of R6G) against a standard calibration curve generated using R6G/MeOH solution, and calculated using the following equations:

$$DLC\ \% = \frac{Weight\ of\ drug\ loaded\ in\ polymeric\ micelles}{Weight\ of\ drug\ loaded\ polymeric\ micelles} \times 100$$

$$DLE\ \% = \frac{Weight\ of\ drug\ loaded\ in\ polymeric\ micelles}{weight\ of\ drug\ input} \times 100$$

Long-term kinetic stability

The structure and stability of R6G-loaded and A-R6G-loaded BU-PPG nanoparticles in aqueous environments were assessed by DLS in the presence of fetal bovine serum (FBS; Thermo Fisher Scientific), which acts as a destabilizing agent. R6G/A-R6G-loaded nanoparticles were mixed with Dulbecco's Modified Eagle Medium (DMEM; pH 7.4, 10 mM; Thermo Fisher Scientific) containing 10% FBS. The variations in the hydrodynamic diameter and distribution of the nanoparticles were monitored over 24 h at 25 °C and 37 °C, respectively.

In vitro drug release assays

In vitro drug release experiments were performed using the dialysis method. Briefly, R6G-loaded and A-R6G-loaded BU-PPG nanoparticles in PBS were placed in 1000 Da cut-off dialysis tubing and dialyzed against large volumes of PBS (10 mM, pH 7.4 and 5.5) with gentle agitation for 48 h at 37 °C or 45 °C. At each time-point (0, 1, 2, 3, 6, 12, 18, 24, 36, and 48 h), an aliquot of dialysis buffer (3 mL) was collected for UV-Vis spectroscopy to quantify the amount of A-R6G (or R6G) released. Fresh PBS (3 mL, pH 5.5 and 7.4) was added to the dialysis tubing to replace the volume of sample removed. The concentrations of R6G/A-R6G were determined by

comparing the absorbance intensity of the collected dialysates against a standard calibration curve. Cumulative A-R6G (or R6G) release from the nanoparticles was determined and plotted as a function of time, using:

$$Cumulative\ drug\ release\ (\%) = \frac{w_t}{w} \times 100$$

where W_t represents the amount of A-R6G (or R6G) released at time t, and W the total amount of R6G/A-R6G loaded into the nanoparticles.

Cell lines and culture conditions

Normal mouse embryonic fibroblast NIH/3T3 cells and human cervical carcinoma HeLa cells (ATCC, Manassas, VA, USA) were maintained in DMEM supplemented with 10% FBS and penicillin-streptomycin at 37 °C in a humidified 5% CO_2 atmosphere. Before the experiments, the cells were detected using trypsin-EDTA and an aliquot was re-suspended in PBS containing 0.1% trypan blue (Thermo Fisher, Waltham, MA, USA) to determine the numbers of cells using a hemocytometer.

In vitro cytotoxicity assays

HeLa cells and NIH/3T3 cells were seeded into 96-well plates at 1×10^6 cells per well in 100 μL media, and incubated with R6G, A-R6G, or R6G-loaded or A-R6G-loaded nanoparticles at various concentrations (0.1–100 μg/mL) for 24 h at 37 °C (pH 7.4), then 20 μL of MTT solution (5 mg/mL) in PBS was added to each well, incubated for 4 h, the media containing unreacted dye was carefully removed, the blue formazan crystals were dissolved in 100 μL dimethyl sulfoxide solution and the absorbance values were determined using a microplate reader (ELx800; BioTek, Winooski, VT, USA) at 570 nm.

Analysis of the cellular localization of R6G-loaded and A-R6G-loaded nanoparticles by confocal laser scanning microscopy (CLSM)

Briefly, HeLa cells and NIH/3T3 cells were seeded into glass-bottomed dishes at an initial density of 2×10^5 cells/well in 2 mL DMEM culture media, incubated for 24 h, washed thrice with PBS and the original media was replaced with fresh DMEM medium at pH 7.4 containing R6G-loaded or A-R6G-loaded nanoparticles. The cells were cultured for 3, 6, 12 or 24 h, washed thrice with PBS, fixed in 4% paraformaldehyde for 30 min, stained using 4',6-diamidino-2-phenylindole DAPI for 15 min to visualize nuclei, washed thrice with PBS and examined by confocal laser scanning microscopy (iRiS™ Digital Cell Imaging System; Logos Biosystems, Gyeonggi-do, South Korea).

Assessment of the cellular uptake of R6G-loaded and A-R6G-loaded nanoparticles by flow cytometry

Approximately 2×10^5 HeLa cells or NIH/3T3 cells were seeded into 6-well plates in DMEM media (2 mL), incubated overnight, then incubated with R6G-loaded or A-R6G-loaded nanoparticles in the culture media at 37 °C for various periods of time (1, 3, 6, 12 or 24 h). The cells were rinsed twice with PBS, detached with 0.25% trypsin-EDTA (0.5 mL, Invitrogen) for 5 min, harvested by centrifugation at 1500 rpm for 3 min, and the cell pellet was washed with PBS and centrifuged, resuspended in ice-cold PBS (0.5 mL) and examined by flow cytometry (FACSAria™ III; BD Biosciences, San Jose, CA, USA). R6G was excited using a 525 nm laser and emitted fluorescence was monitored at 550 nm.

Assessment of apoptotic and necrotic cell death

The pathways of cell death induced by R6G-loaded and A-R6G-loaded nanoparticles in HeLa cells and NIH/3T3 cells were evaluated by flow cytometry (FACSAria™ III, BD Biosciences, San Jose, CA, USA) using the BV421 Annexin V and Ghost Dye™ Red 780 (GDR780) Detection Kit.[38,39] Approximately 2×10^5 HeLa cells or NIH/3T3 cells were seeded into 6-well plates in DMEM (2 mL), incubated overnight, then treated with the drug-loaded nanoparticles in culture media (2 mL) for various periods of time (1, 3 and 6 h). After incubation, the cells were rinsed in PBS, detached using 0.25% trypsin-EDTA, centrifuged at 1500 rpm for 3 min, the cell pellets were washed with PBS, centrifuged, and the cells were resuspended in binding buffer (100 μL) in flow cytometer tubes. GDR780 (1 μL) was added and the cell suspension was incubated in the dark at room temperature for 15 min, then BV421 Annexin V (5 μL) was added and incubated in the dark at room temperature for 30 min, and then binding buffer (400 μL) was added and the cells were analyzed by flow cytometry (FACSAria™ III, BD Biosciences). Untreated cultured cells were used as control group for background correction.

Statistical analysis

Each experiment was performed in triplicate and was repeated at least three times; the mean ± standard error (± SD) values are reported.

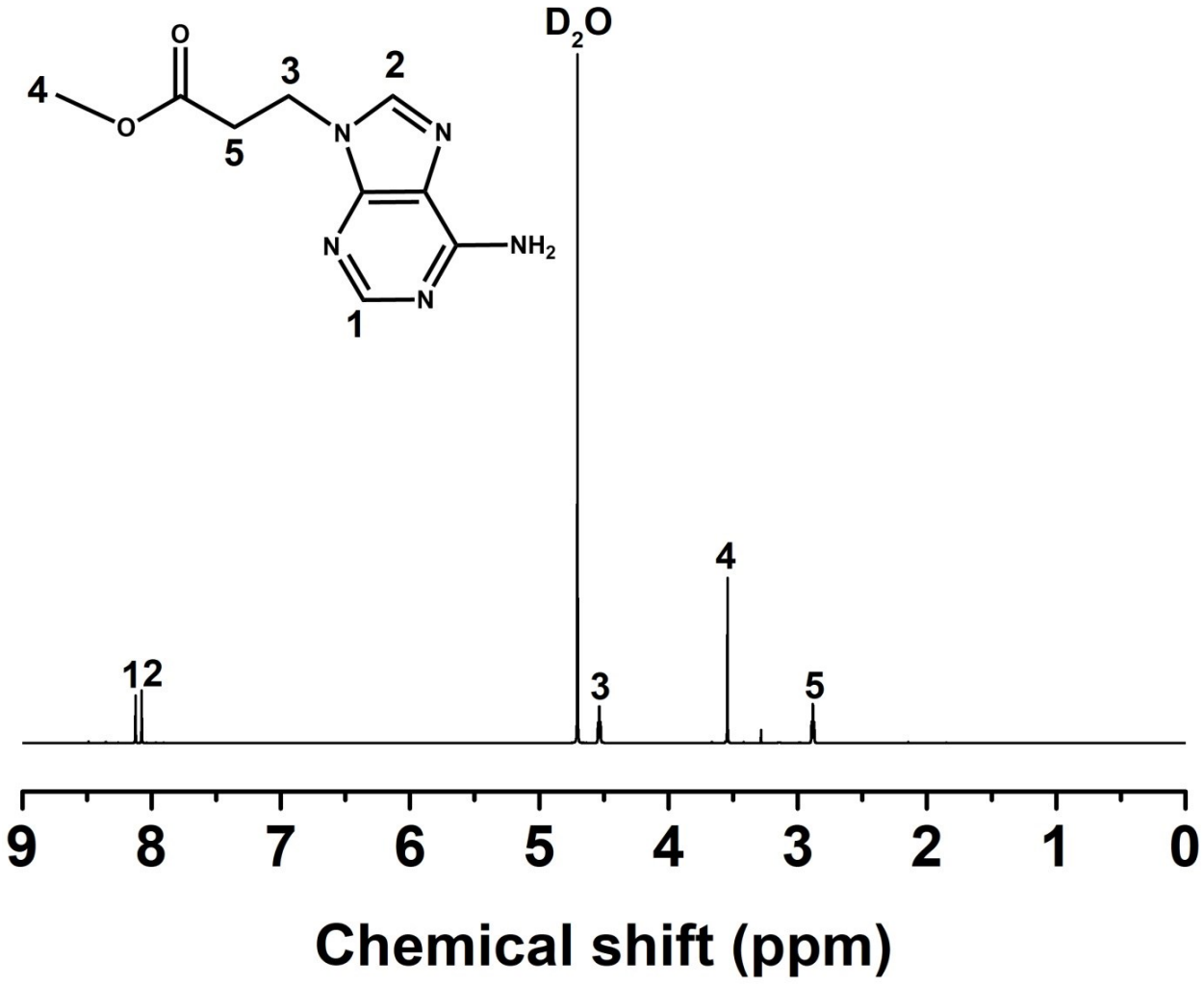

Fig. S1: ^{1}H NMR spectrum of A-MA in deuterium oxide (D_2O).

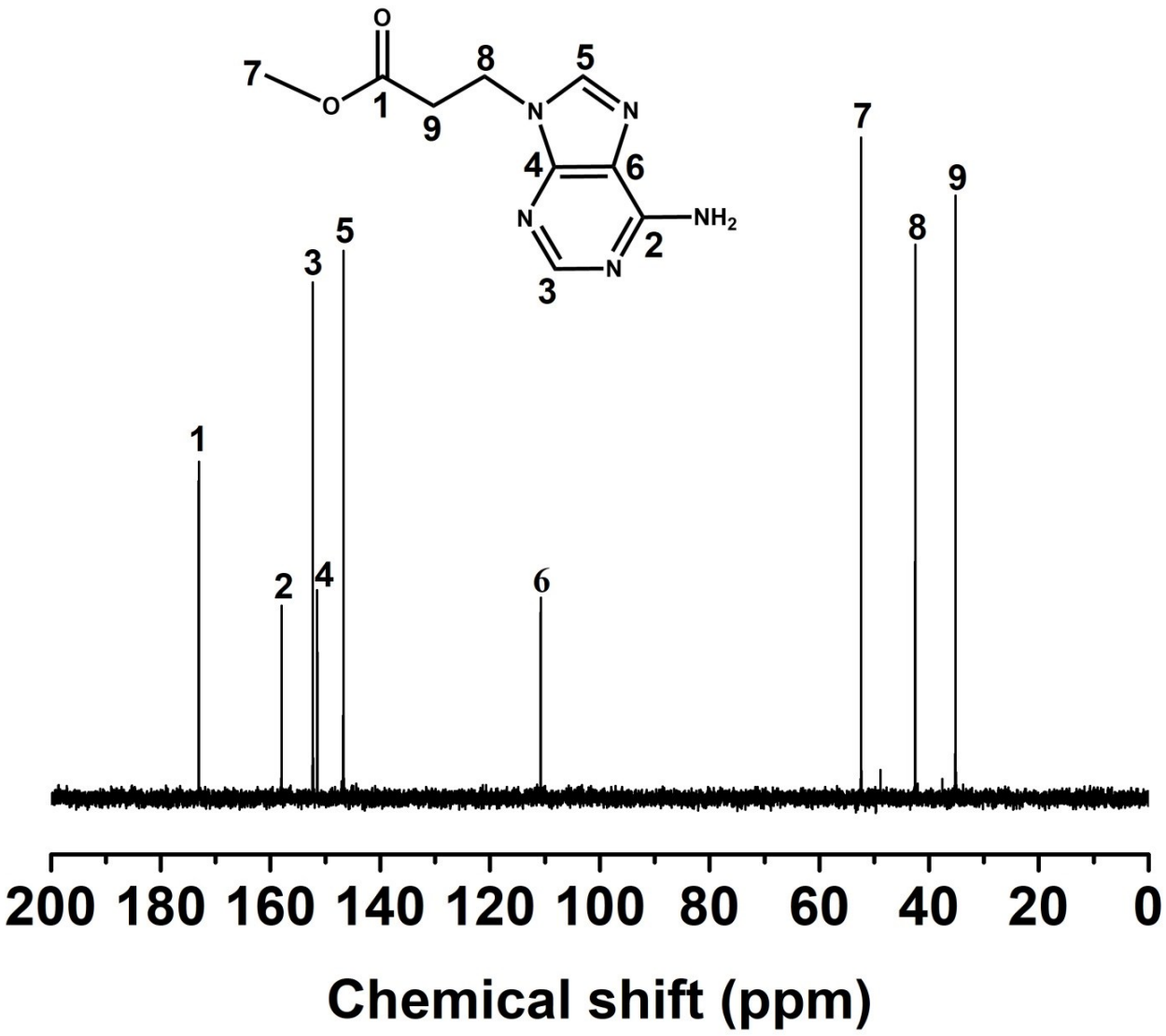

Fig. S2: ^{13}C NMR spectrum of A-MA in D_2O.

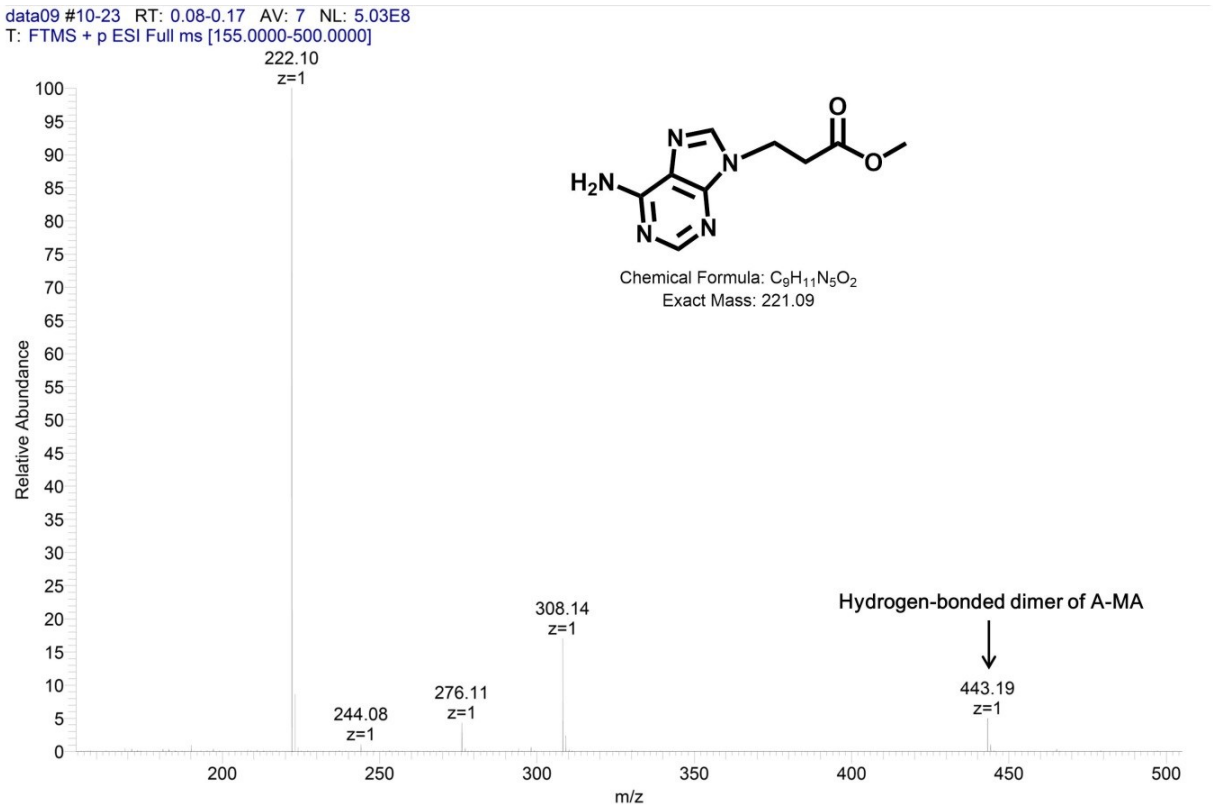

Fig. S3: Mass spectrum of A-MA.

Table S1: Elemental content of A-MA, A-Propylamine and A-R6G.

Compound		N (%)	C (%)	H (%)
A-MA	Found	29.886	49.195	5.011
	Theory	31.664	48.861	5.012
A-Propylamine	Found	33.662	45.977	6.613
	Theory	37.244	50.182	6.511
A-R6G	Found	18.086	63.722	6.371
	Theory	18.113	63.832	6.083

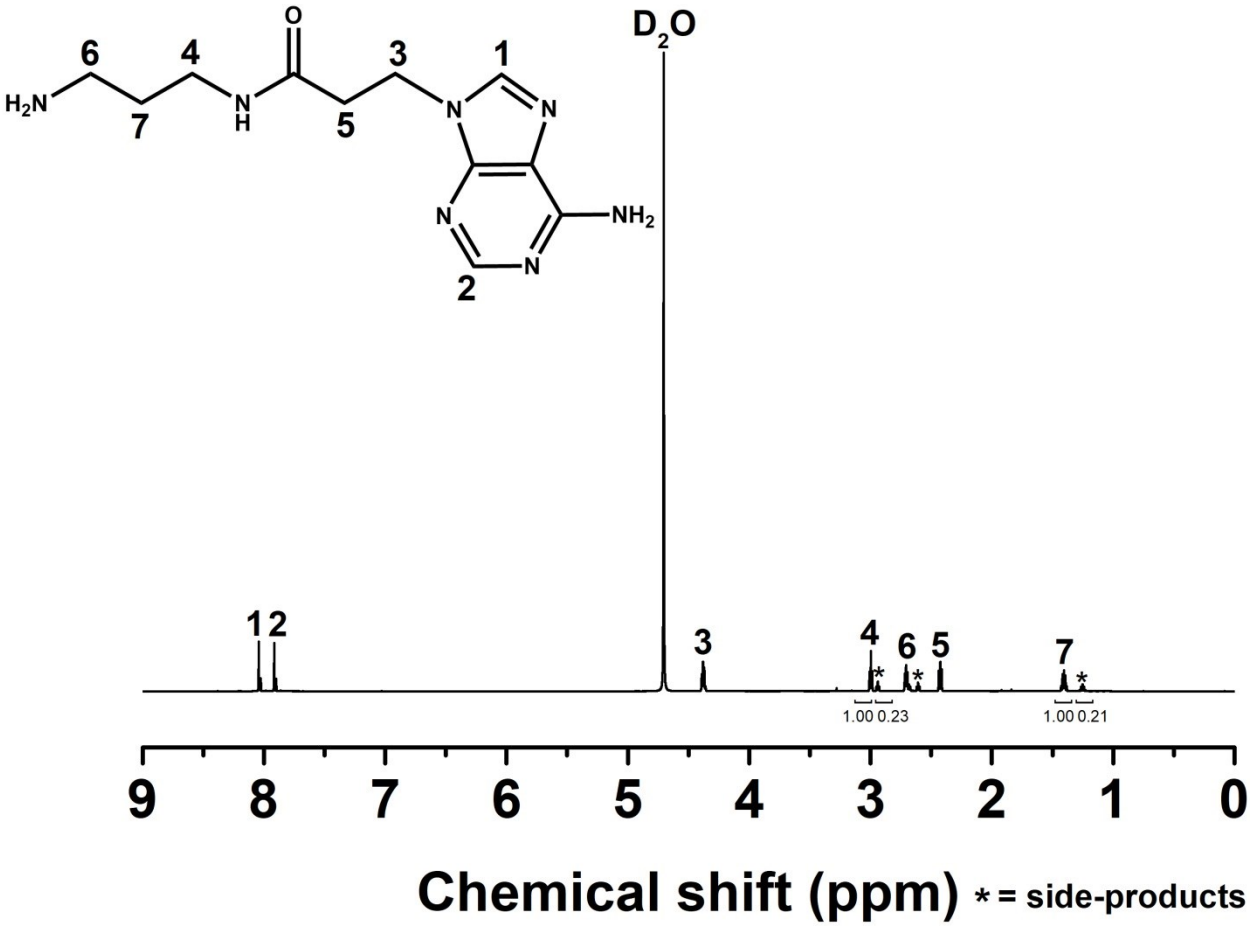

Fig. S4: ^{1}H NMR spectrum of A-Propylamine in D_2O. The A-Propylamine intermediate still contains some impurities, which may majorly be contributed by the formation of the bisadenine byproduct. However, this reaction still dominates the formation and production of A-Propylamine and can form more than 75% of A-Propylamine based on the integral ratio of proton signals in NMR spectroscopy.

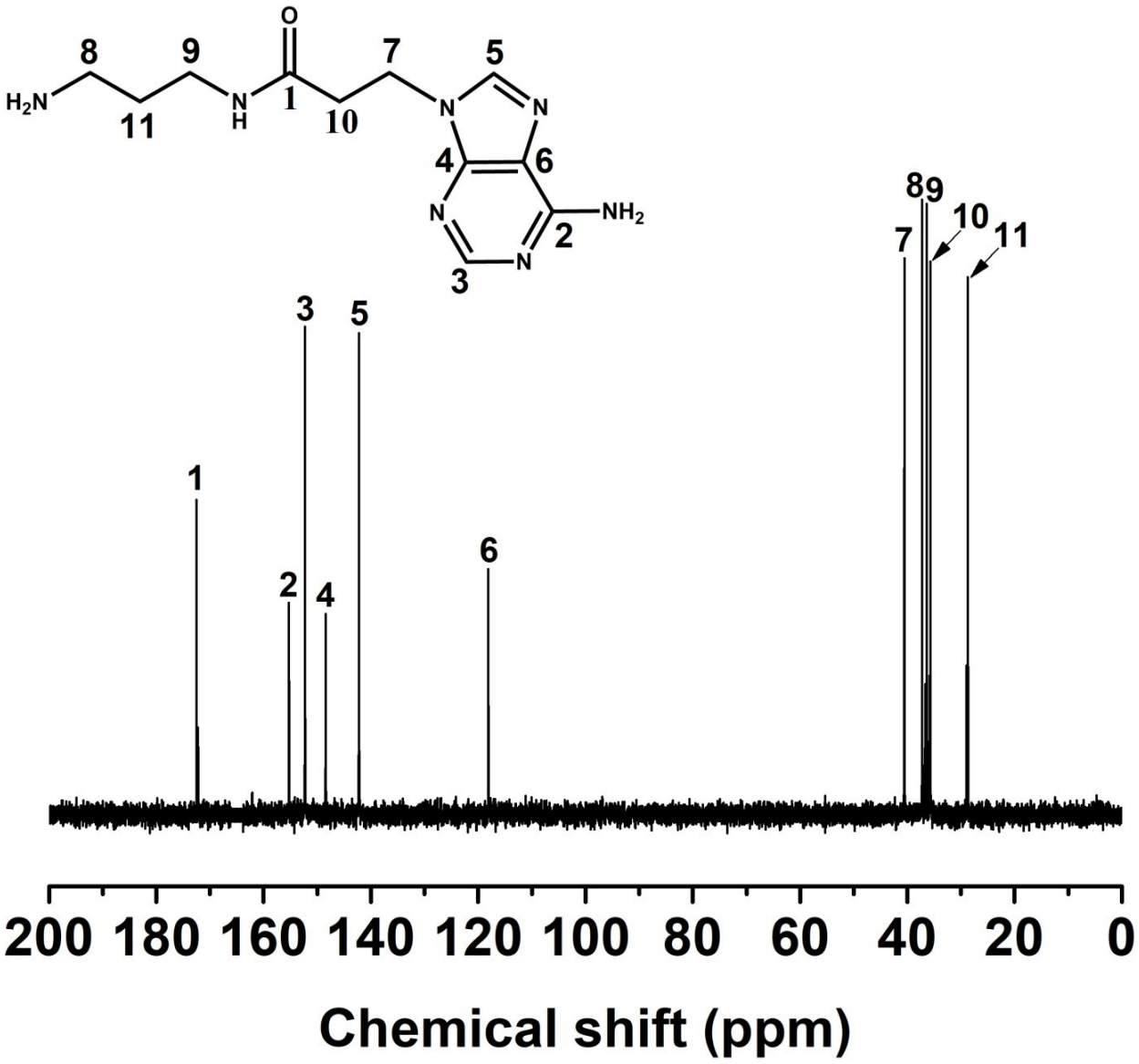

Fig. S5: ^{13}C NMR spectrum of A-Propylamine in D_2O.

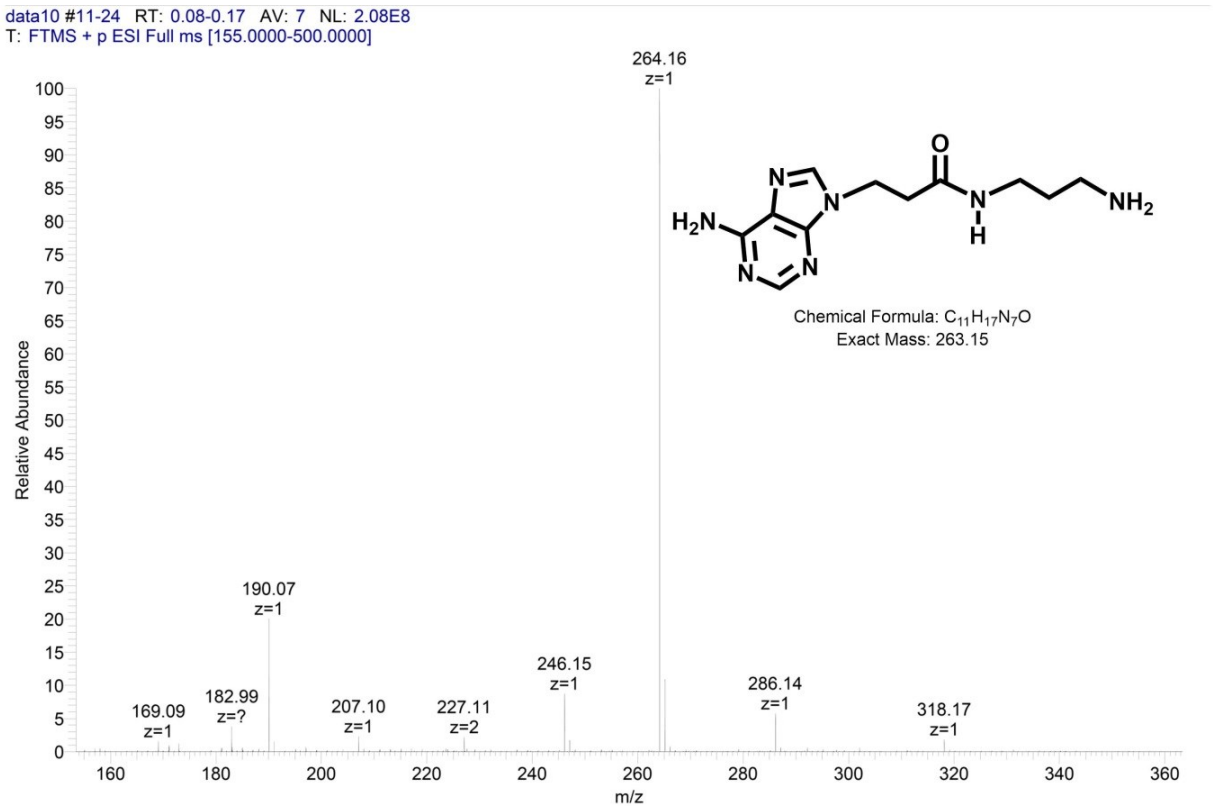

Fig. S6: Mass spectrum of A-Propylamine.

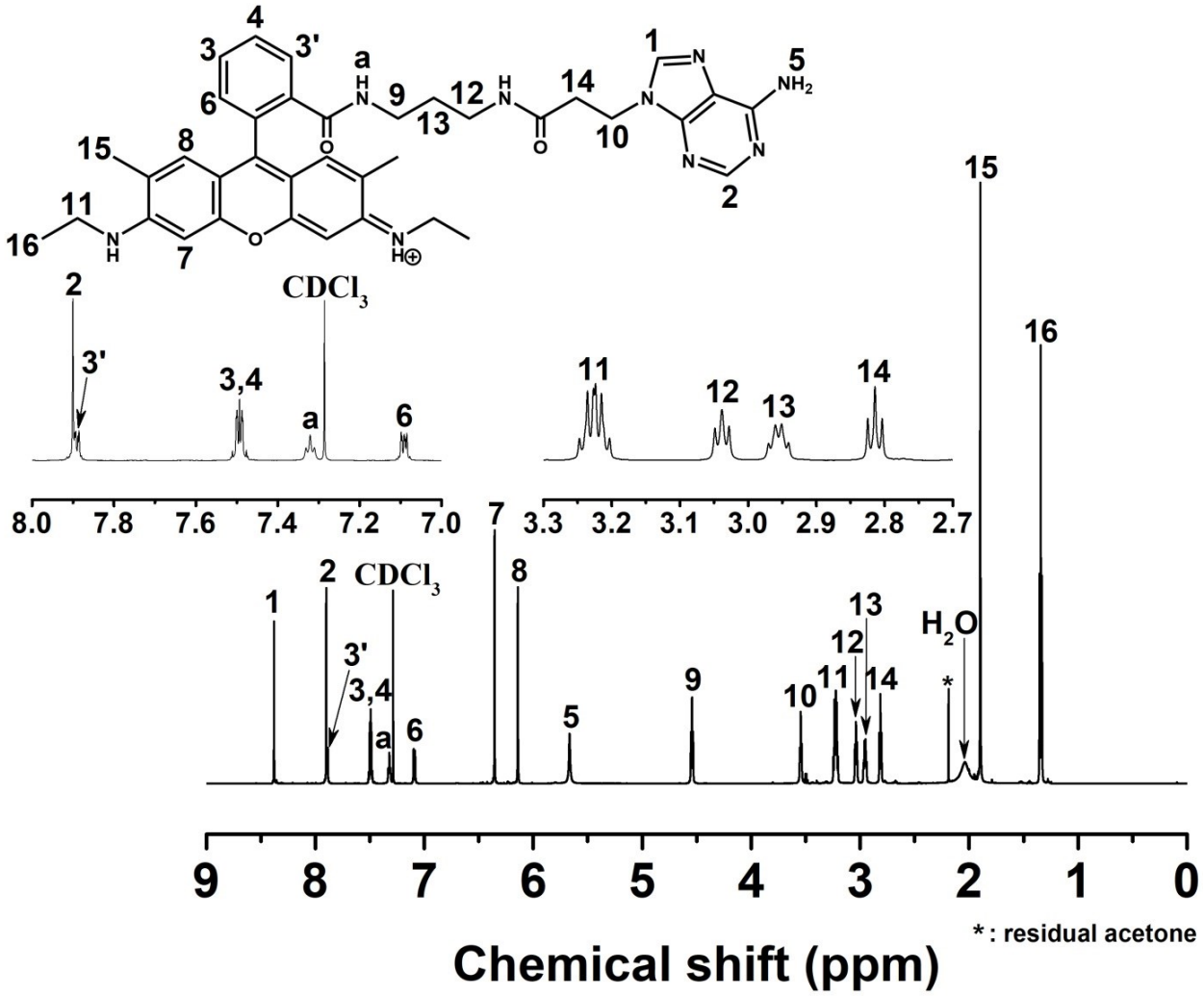

Fig. S7a: ^{1}H NMR spectrum of A-R6G in deuterated chloroform ($CDCl_3$).

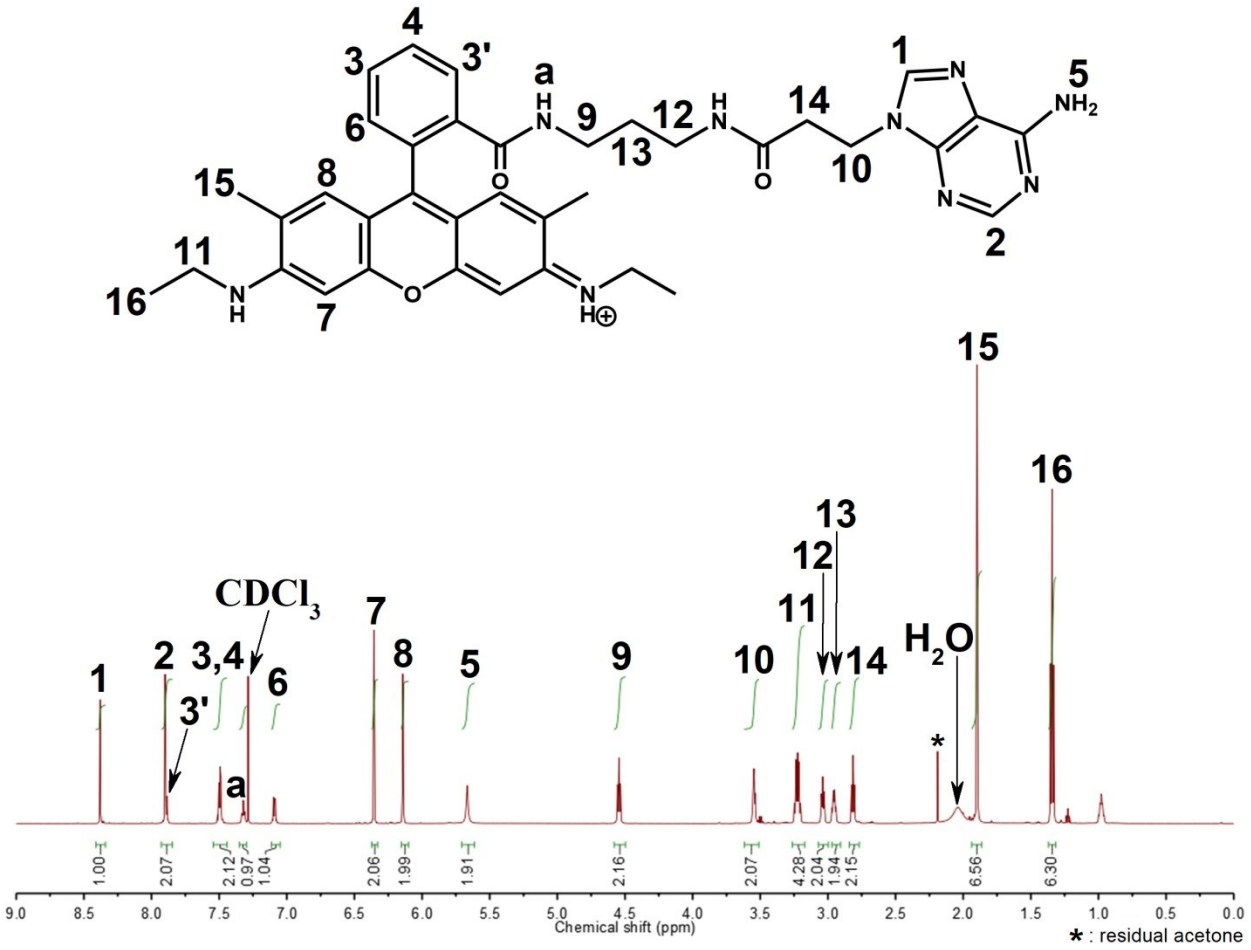

Fig. S7b: Integration values for the peaks in the ^{1}H NMR spectrum of A-R6G in $CDCl_3$.

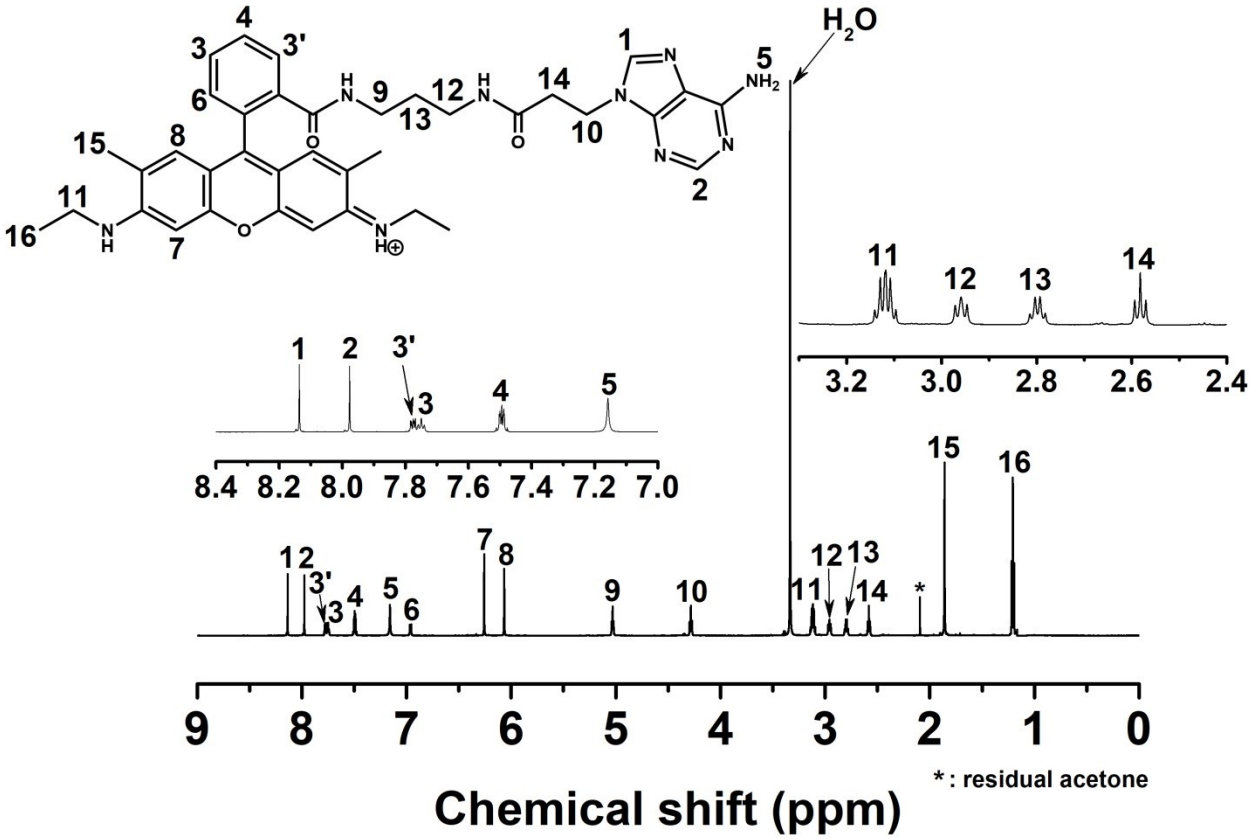

Fig. S8a: ^{1}H NMR spectrum of A-R6G in deuterated dimethyl sulfoxide (DMSO-d_6).

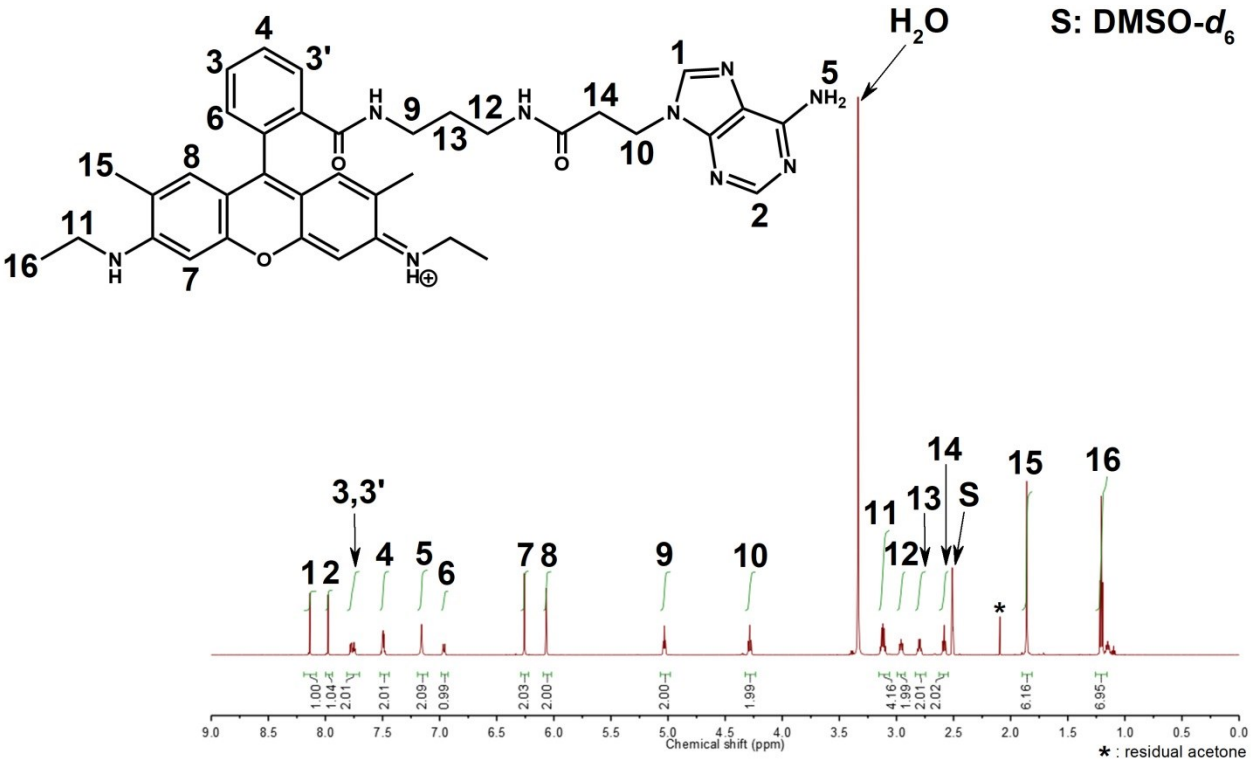

Fig. S8b: Integration values for the peaks in the ^{1}H NMR spectrum of A-R6G in DMSO-d_6.

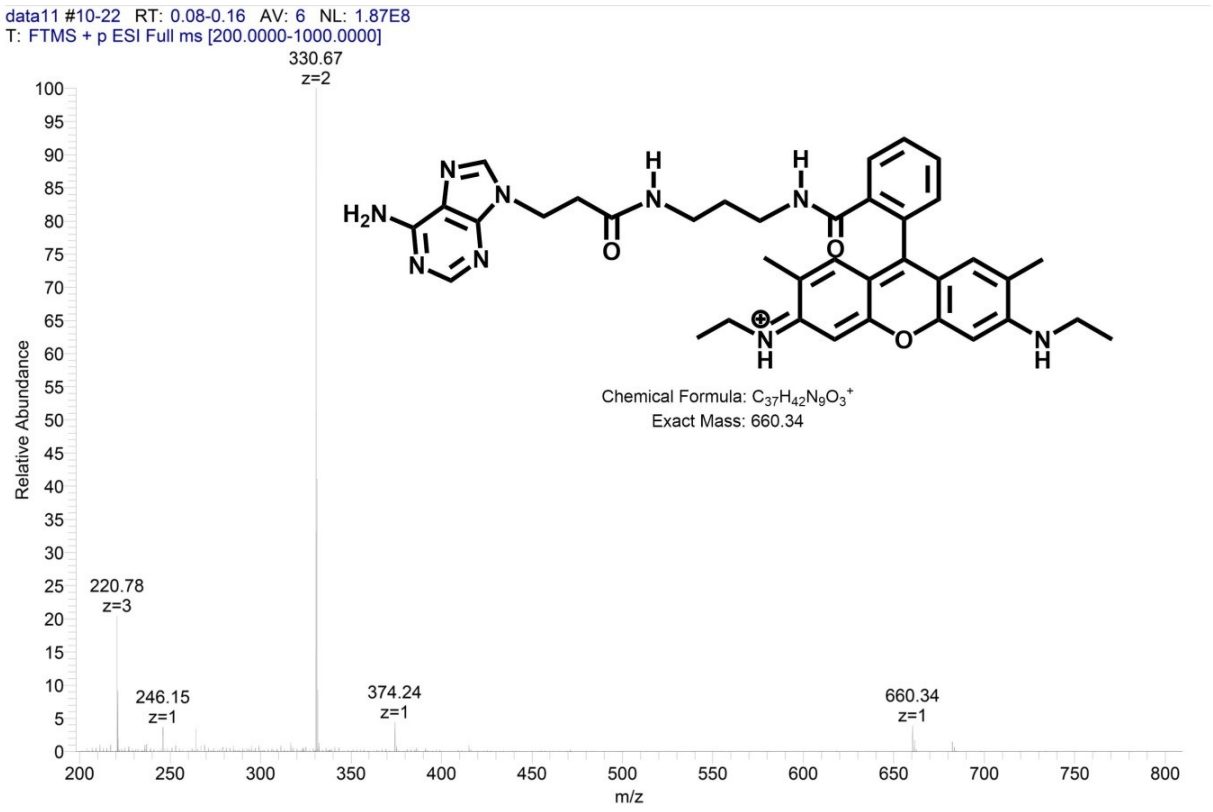

Fig. S9: Mass spectrum of A-R6G.

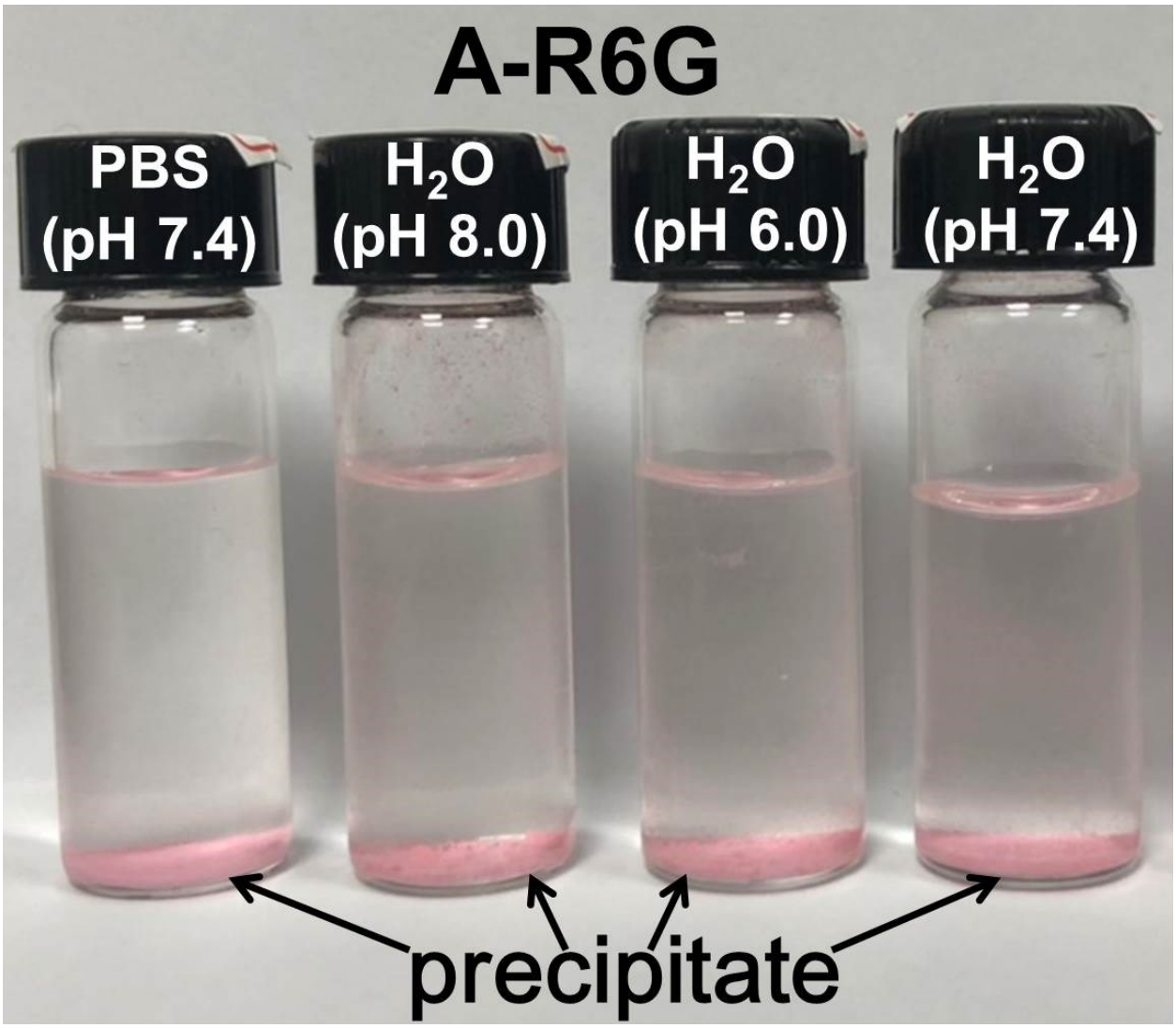

Fig. S10: Photograph of A-R6G in PBS (pH 7.4) and aqueous solutions of various pH values after heating at 70 °C for 1 d and standing at 25 °C for 12 h.

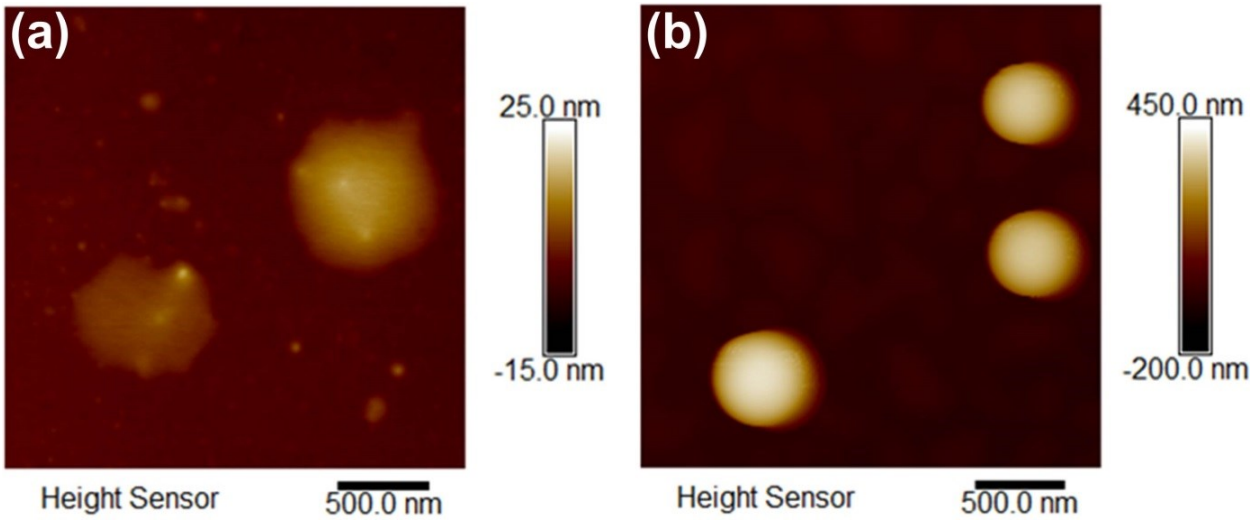

Fig. S11: AFM images of spin-coated **(a)** R6G and **(b)** A-R6G thin films at 25 °C.

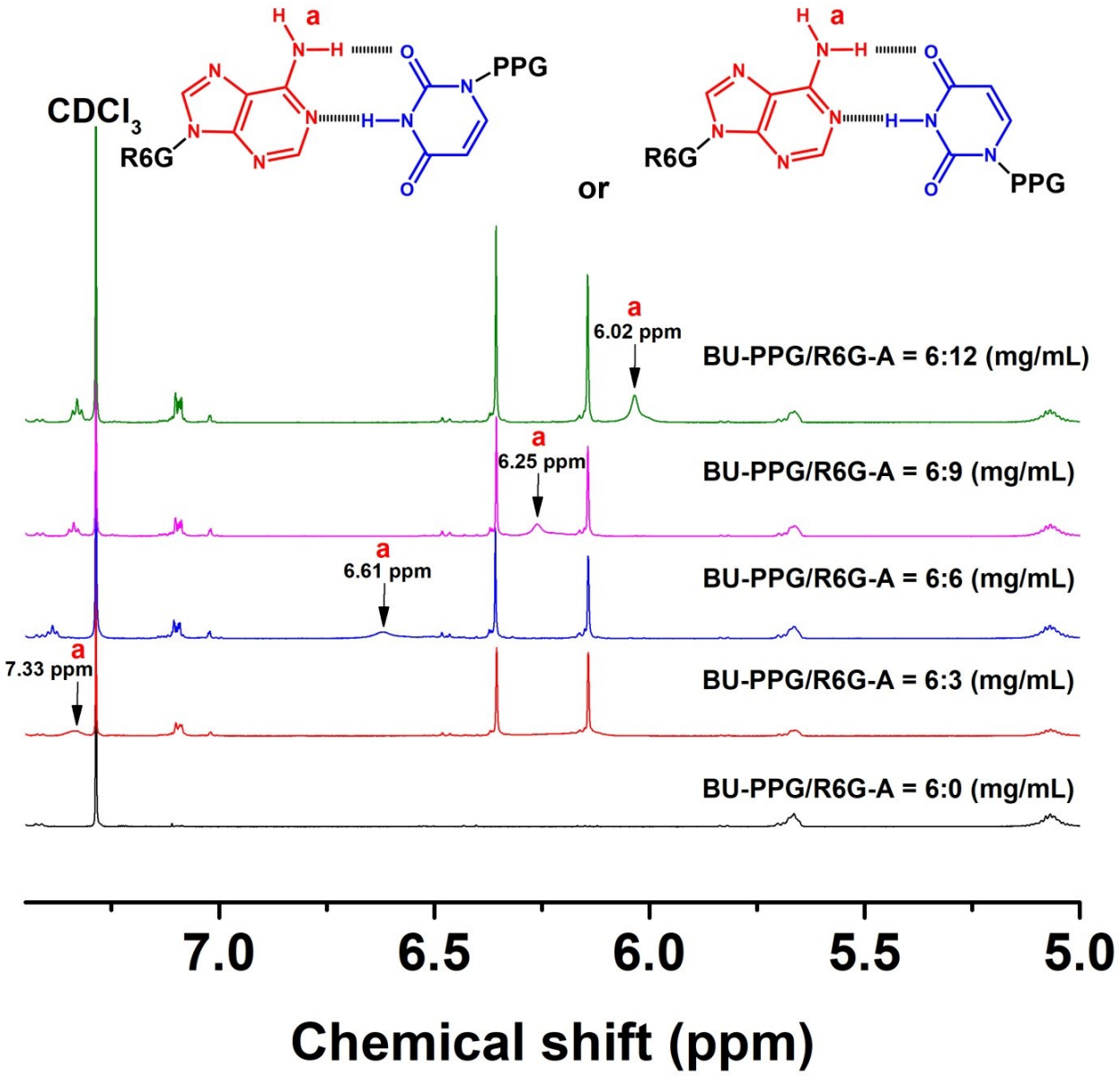

Fig. S12: ^{1}H NMR spectra obtained from ^{1}H NMR titration experiments of A-R6G/BU-PPG complexes in $CDCl_3$ at 25 °C. The NH_2 region of the ^{1}H-NMR spectra of A-R6G after blending with BU-PPG is indicated.

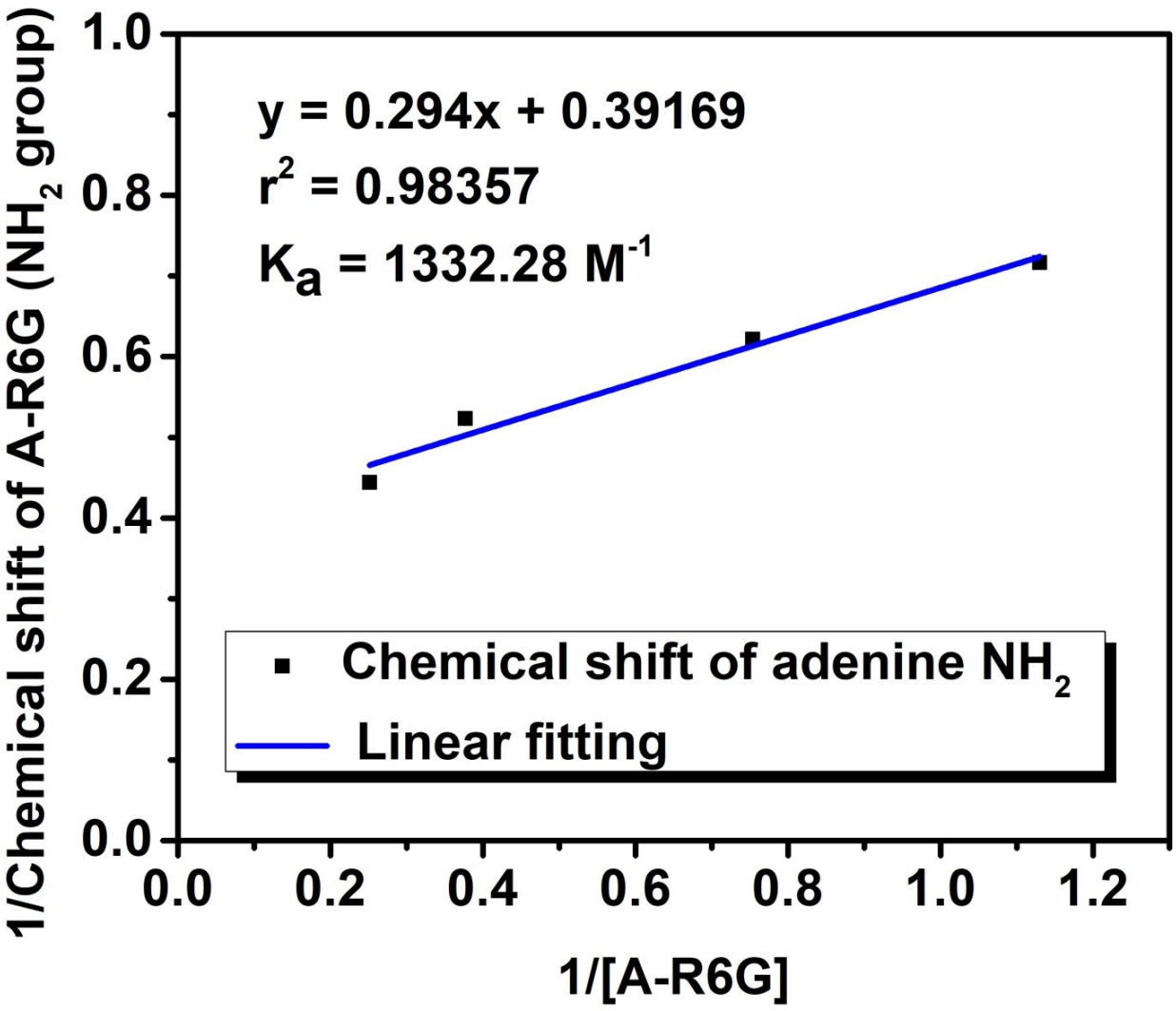

Fig. S13: Benesi-Hildebrand plots for the A-R6G/BU-PPG association in $CDCl_3$ at 25 °C.

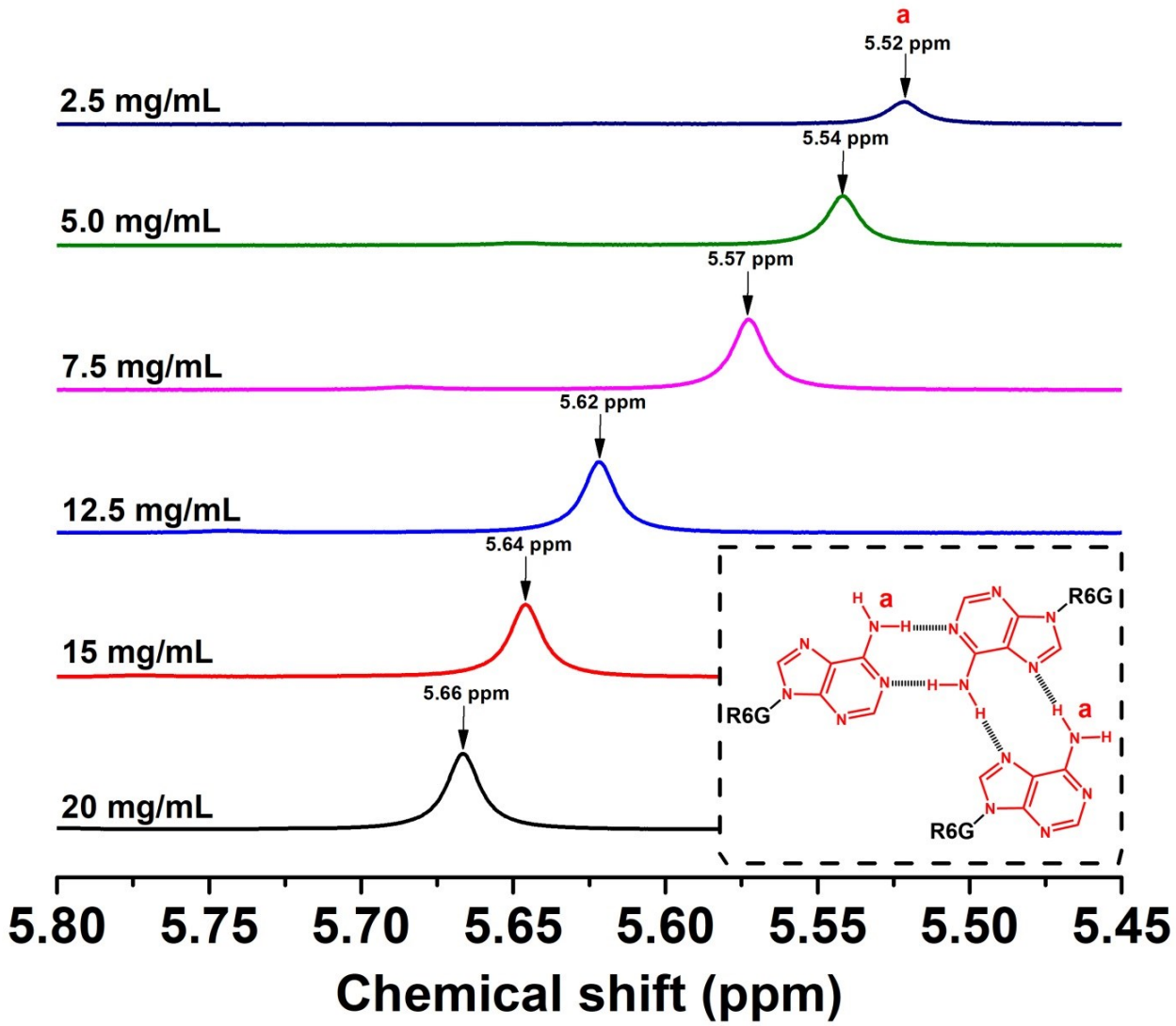

Fig. S14: ^{1}H NMR spectra of various concentrations of A-R6G in $CDCl_3$ at 25 °C. The NH_2 region of the ^{1}H-NMR spectrum of A-R6G is indicated.

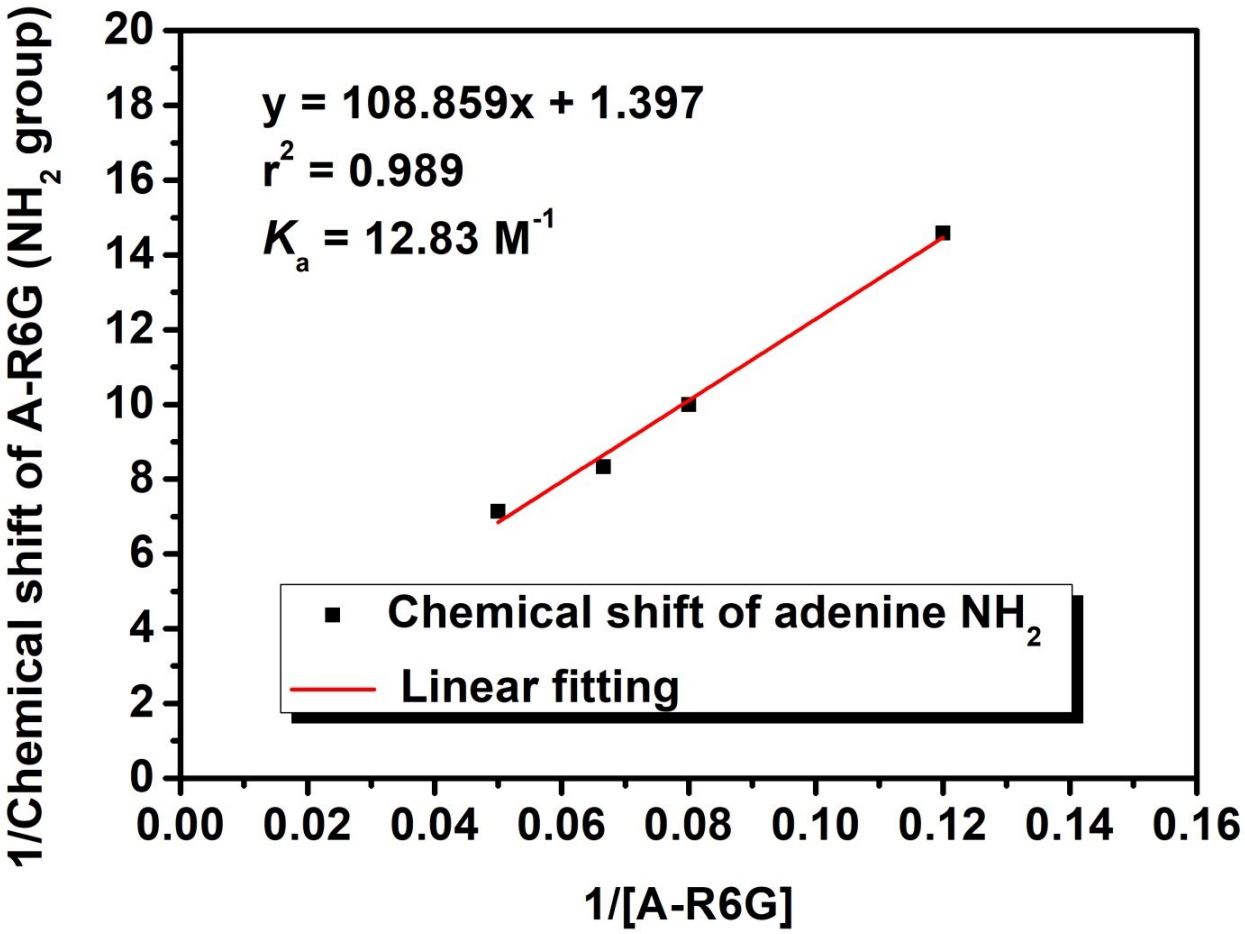

Fig. S15: Benesi-Hildebrand plots for the A-R6G association in $CDCl_3$ at 25 °C.

Table S2: Drug loading content (DLC) and encapsulation efficiency (EE) of A-R6G-loaded and R6G-loaded BU-PPG nanoparticles.

Carrier:Drug (mg:mg)	**R6G/BU-PPG**		**A-R6G/BU-PPG**	
	DLC (*wt*%)	**EE (*wt*%)**	**DLC (*wt*%)**	**EE (*wt*%)**
1.0:0.1	10.17	81.32	55.32	98.47
1.0:0.2	13.24	68.18	69.63	90.51
1.0:0.3	17.78	62.83	73.06	85.24
1.0:0.6	22.14	49.82	78.04	76.74
1.0:1.0	23.62	44.87	84.28	72.48

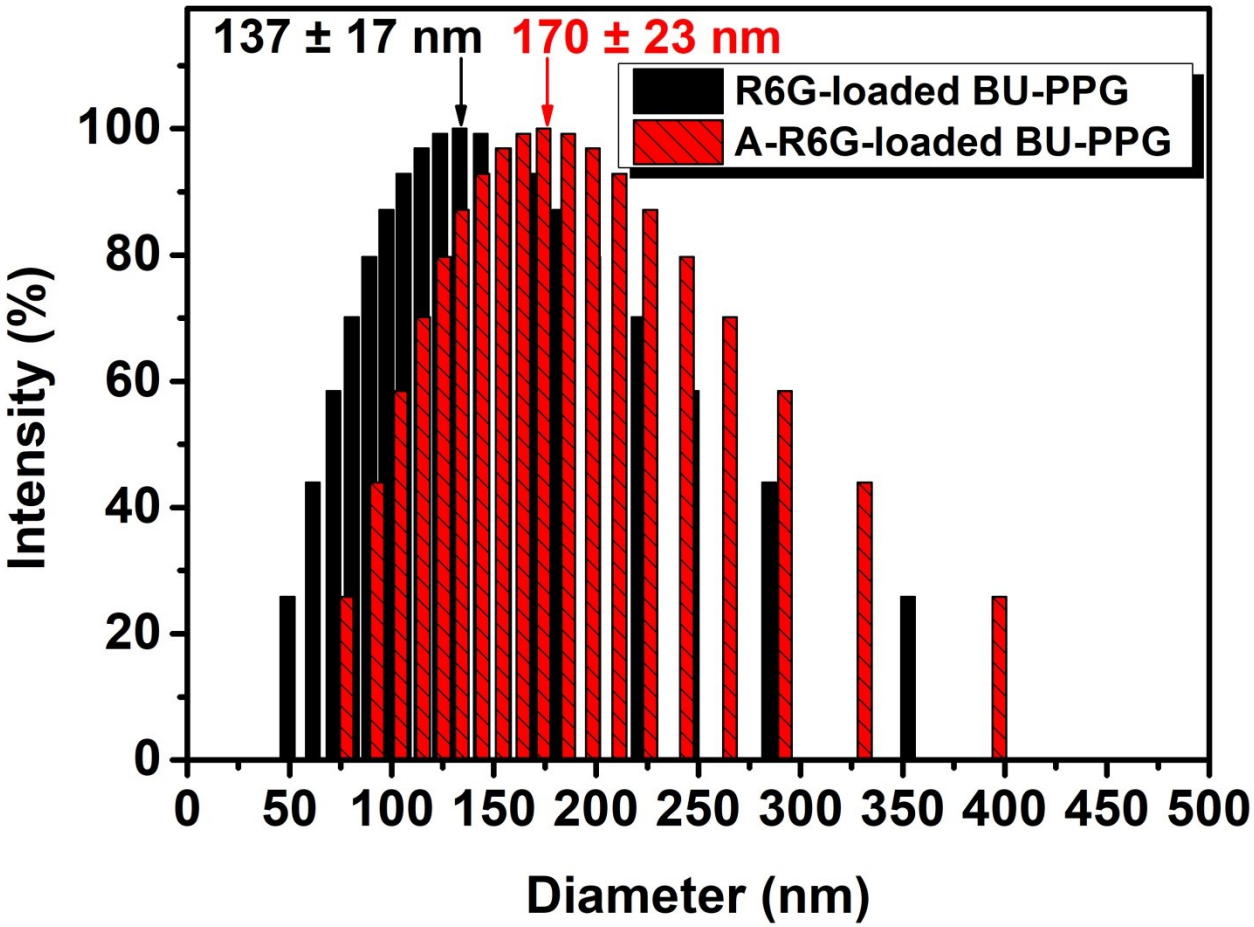

Fig. S16: DLS intensity mean size distribution curves for A-R6G-loaded and R6G-loaded BU-PPG nanoparticles in aqueous solution.

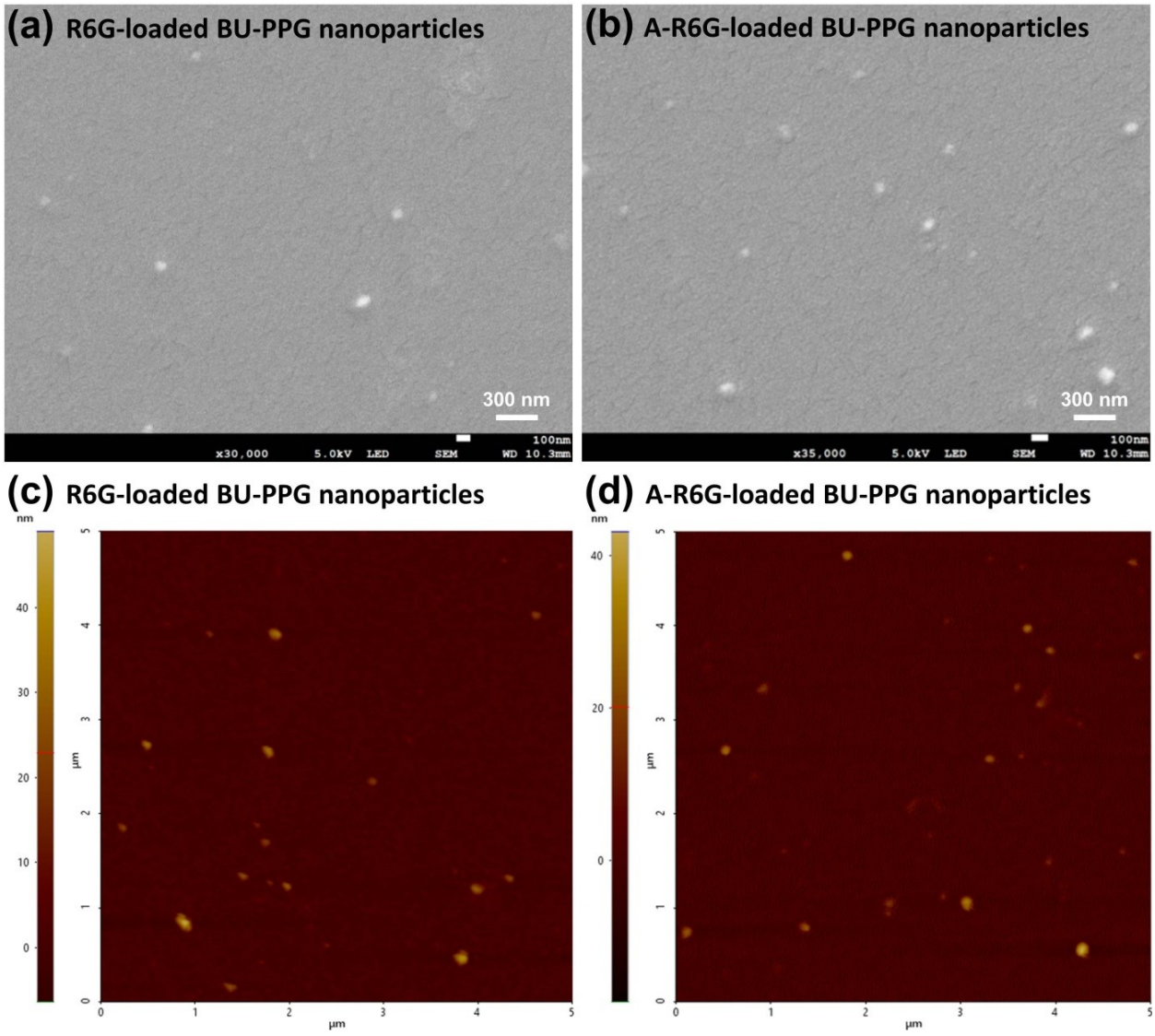

Fig. S17: SEM and AFM images of spin-coated A-R6G-loaded and R6G-loaded BU-PPG films at 25 °C.

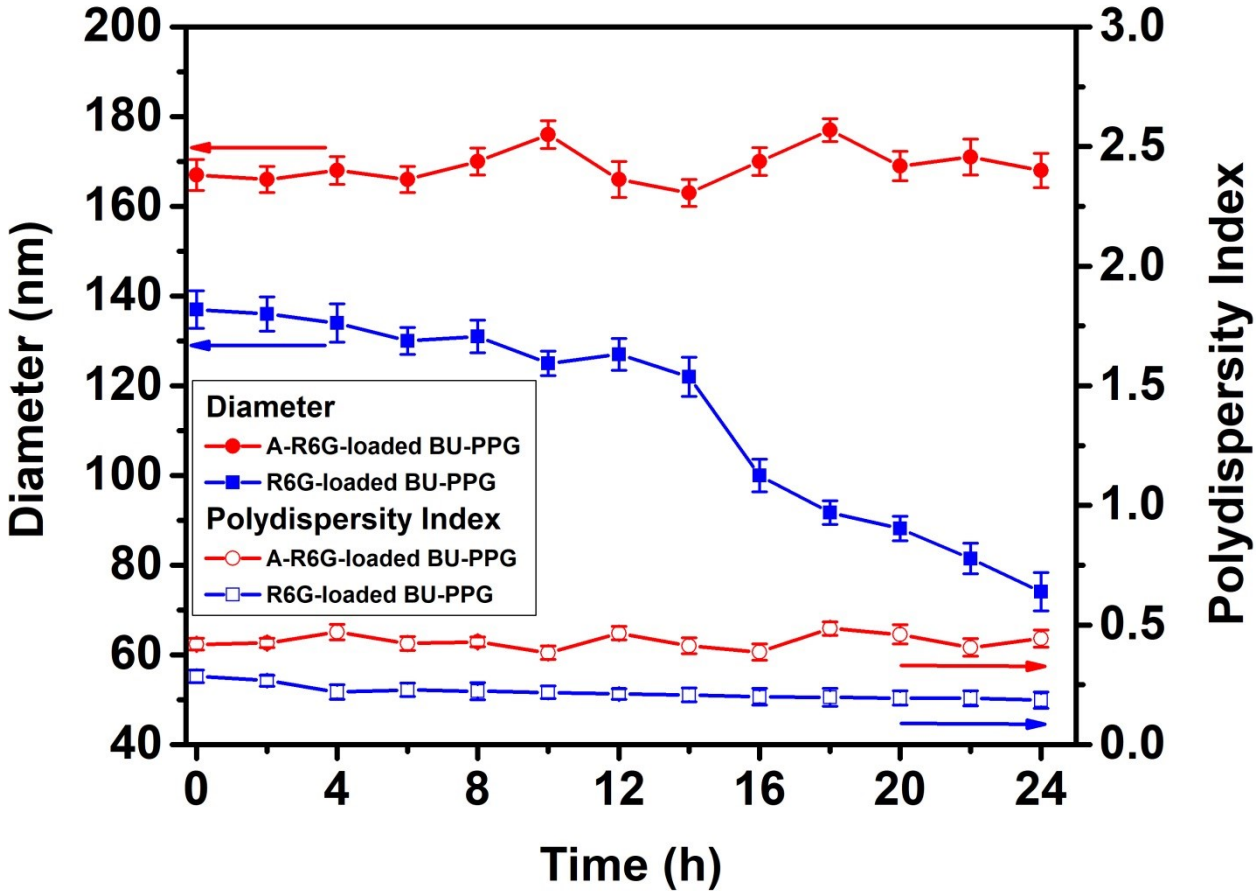

Fig. S18: Time-dependent DLS measurements of the kinetic stability of A-R6G-loaded and R6G-loaded BU-PPG nanoparticles in DMEM media containing 10% (v/v) FBS at 37 ° C.

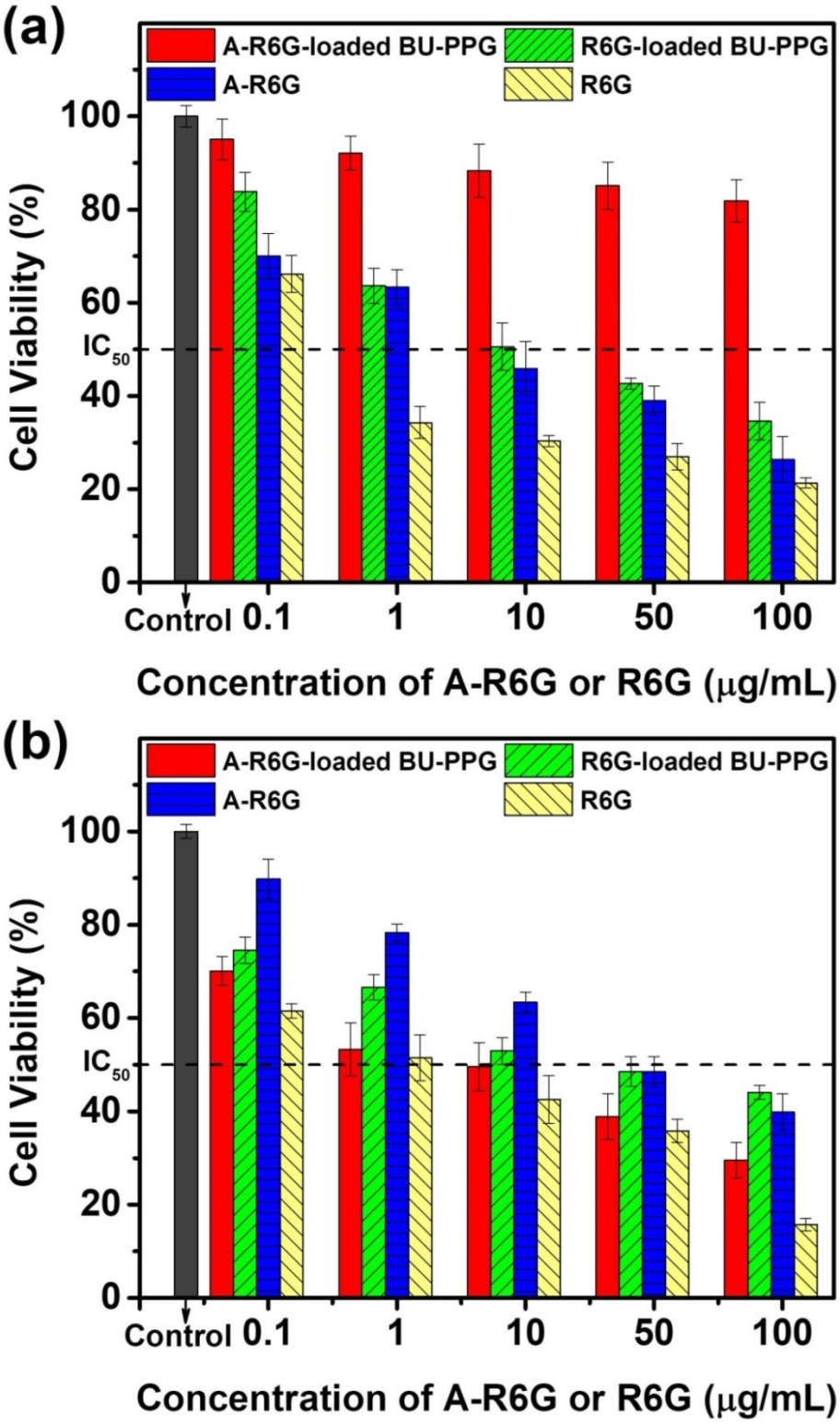

Fig. S19: MTT cell viability assays of **(a)** NIH/3T3 cells and **(b)** HeLa cells after incubation with various concentrations of A-R6G-loaded and R6G-loaded BU-PPG nanoparticles for 24 h.

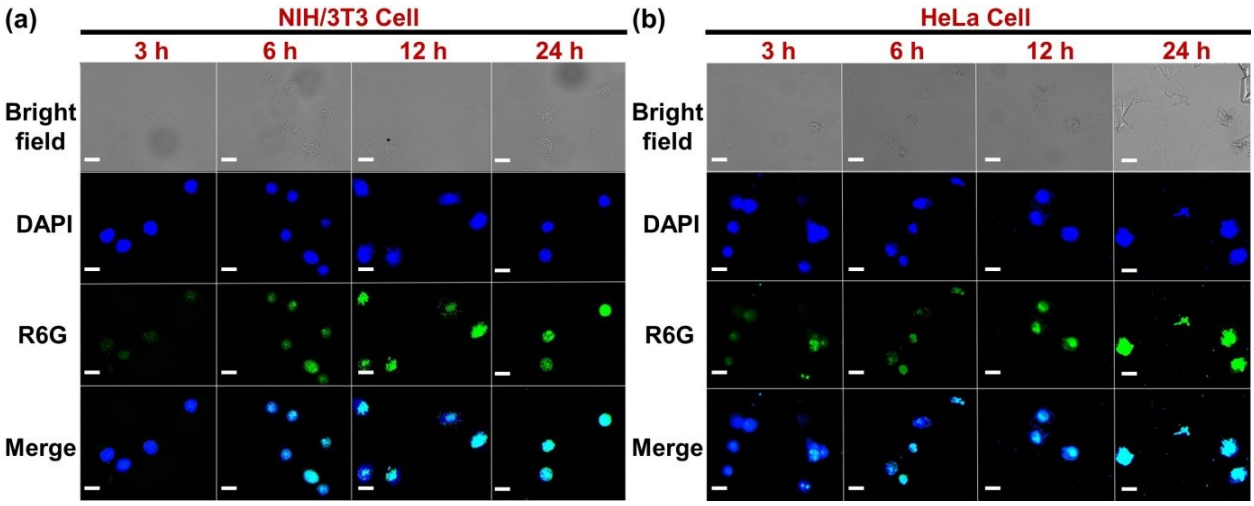

Fig. S20: CLSM fluorescence images of **(a)** NIH/3T3 and **(b)** HeLa cells incubated with R6G-loaded BU-PPG nanoparticles at pH 7.4 and 37 °C for various periods of time. The white scale bars in all CLSM images represent 20 μm.

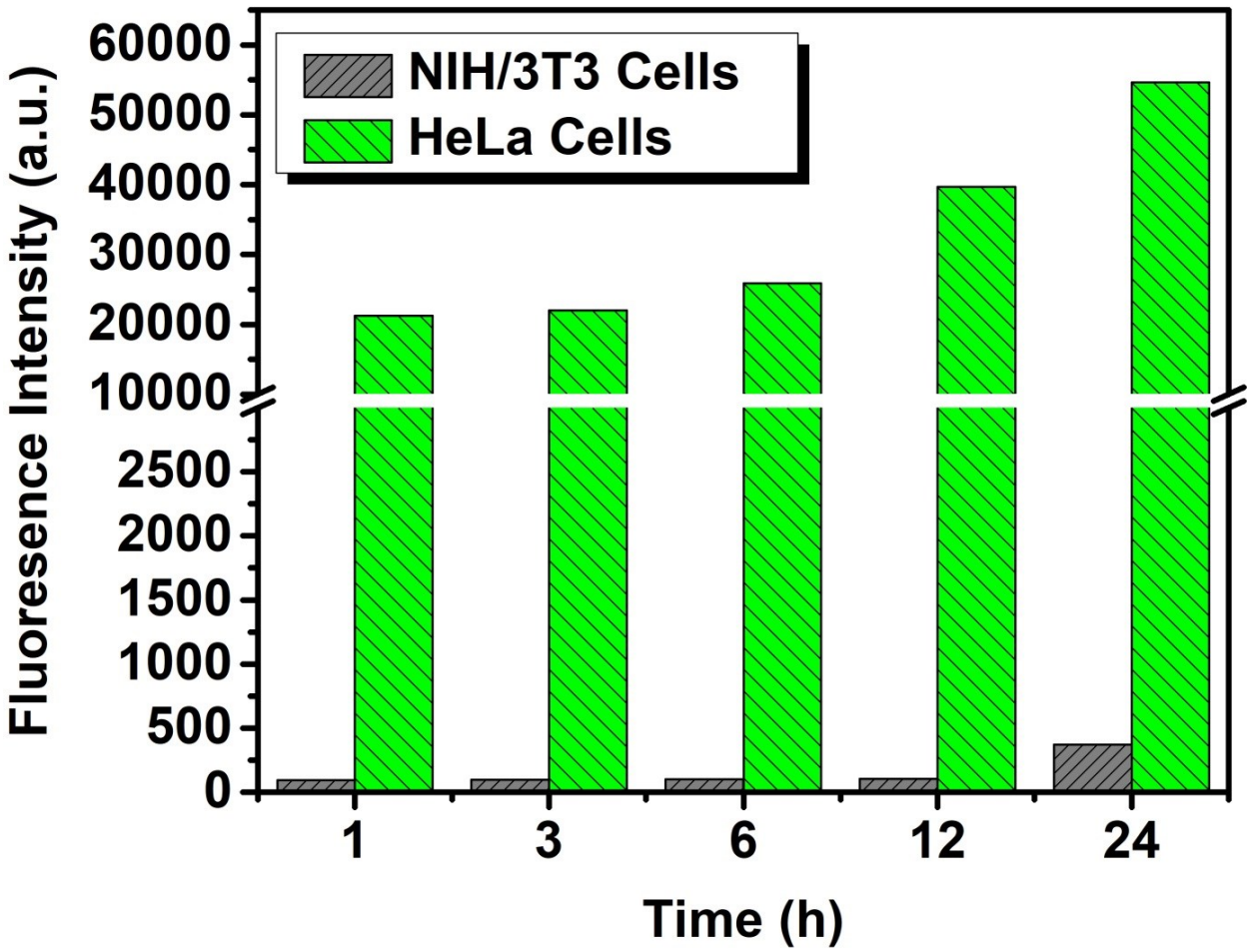

Fig. S21: Fluorescence intensities of NIH/3T3 cells and HeLa cells after incubation with A-R6G-loaded BU-PPG nanoparticles at pH 7.4 and 37 °C for various periods of time.